Coalescence as the origin of nuclear clusters

Ulrich Heinz

THE OHIO STATE UNIVERSITY

presented (via Zoom) at

Origin of nuclear clusters in hadronic collisions

CERN, May 19-20, 2020

Unterstützt von / Supported by

Alexander von Humboldt
Stiftung/Foundation

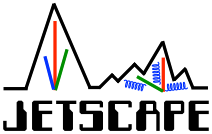

Coalescence, flow, HBT, and all that ...

Prologue

- Coalescence model for the production of light nuclei in high energy hadron-hadron and hadron-nucleus collisions (cosmic rays) first introduced in the 1960s:

  Hagedorn 1960,1962,1965; Butler & Pearson 1963; Schwarzschild & Zupančič 1963

Prologue

- Coalescence model for the production of light nuclei in high energy hadron-hadron and hadron-nucleus collisions (cosmic rays) first introduced in the 1960s:

  Hagedorn 1960,1962,1965; Butler & Pearson 1963; Schwarzschild & Zupančič 1963

- Further development in the 1970s and 80s motivated by first experimental results with heavy-ion collisions at the BEVALAC (Gutbrod et al. 1976):

  Bond, Johansen, Koonin, Garpmann 1977; Mekjian 1977, 1978; Kapusta 1980, Sato & Yazaki 1981; Remler 1981, Gyulassy, Frankel & Remler 1983; Csernai & Kapusta 1986; Mrówczynski 1987; Dover et al. 1991

Prologue

- Coalescence model for the production of light nuclei in high energy hadron-hadron and hadron-nucleus collisions (cosmic rays) first introduced in the 1960s:

  Hagedorn 1960,1962,1965; Butler & Pearson 1963; Schwarzschild & Zupančič 1963

- Further development in the 1970s and 80s motivated by first experimental results with heavy-ion collisions at the BEVALAC (Gutbrod et al. 1976):

  Bond, Johansen, Koonin, Garpmann 1977; Mekjian 1977, 1978; Kapusta 1980, Sato & Yazaki 1981; Remler 1981, Gyulassy, Frankel & Remler 1983; Csernai & Kapusta 1986; Mrówczynski 1987; Dover et al. 1991

- Long initial discussions about the interpretation of the "invariant coalescence factor" B_A defined by

$$E_A \frac{dN_A}{d^3P_A} = B_A \left(E_\mathrm{p} \frac{dN_\mathrm{p}}{d^3P_\mathrm{p}} \right)^Z \left(E_\mathrm{n} \frac{dN_\mathrm{n}}{d^3P_\mathrm{n}} \right)^N \Bigg|_{P_\mathrm{p}=P_\mathrm{n}=P_A/A} .$$

  (1) "momentum-space coalescence volume" (Butler & Pearson, Schwarzschild & Zupančič, Gutbrod et al.);
  (2) "inverse fireball volume" $B_A \sim V^{A-1}$ (Bond et al, Mekjian).

Prologue

- The 1980s saw an increased focus on the phase-space and quantum mechanical aspects of nuclei formation through coalescence. An important paper by Danielewicz & Schuck 1992 used quantum kinetic theory to allow for scattering by a 3rd body to account for energy conservation in deuteron formation. Scheibl & Heinz 1999 used their work to derive a generalized Cooper-Frye formula for nuclear cluster spectra from coalescence,

$$E\frac{d^3N_A}{d^3P} = \frac{2J_A+1}{(2\pi)^3}\int_{\Sigma_f} P\cdot d^3\sigma(R)\, f_p^Z(R,P/A)\, f_n^N(R,P/A)\, \mathcal{C}_A(R,P),$$

where the "quantum mechanical correction factor" $\mathcal{C}_A(R,P)$, first introduced by Hagedorn 1960, accounts for the suppression of the coalescence probability in small or rapidly expanding fireballs where the cluster wave function may not fit inside the "homogeneity volume" of nucleons with similar momenta that contribute to the coalescence.

Prologue

- The 1980s saw an increased focus on the phase-space and quantum mechanical aspects of nuclei formation through coalescence. An important paper by Danielewicz & Schuck 1992 used quantum kinetic theory to allow for scattering by a 3rd body to account for energy conservation in deuteron formation. Scheibl & Heinz 1999 used their work to derive a generalized Cooper-Frye formula for nuclear cluster spectra from coalescence,

$$E\frac{d^3N_A}{d^3P} = \frac{2J_A+1}{(2\pi)^3}\int_{\Sigma_f} P\cdot d^3\sigma(R)\, f_p^Z(R,P/A)\, f_n^N(R,P/A)\, \mathcal{C}_A(R,P),$$

  where the "quantum mechanical correction factor" $\mathcal{C}_A(R,P)$, first introduced by Hagedorn 1960, accounts for the suppression of the coalescence probability in small or rapidly expanding fireballs where the cluster wave function may not fit inside the "homogeneity volume" of nucleons with similar momenta that contribute to the coalescence.
- A direct connection between deuteron coalescence and femtoscopic 2-particle correlations (intensity interferometry) was first noted in Mrówczynski 1987-93 and recently made even more explicit by Blum & Takimoto 2019.
  Working it out explicitly in a semi-realistically parametrized expanding fireball model, Scheibl & Heinz 1999 found the following main results:

Coalescence, flow, HBT, and all that ...

Main results: 1. The quantum mechanical correction factor

The quantum mechanical correction factor (approximately independent of position) averaged over the freeze-out surface is given by (Scheibl & Heinz 1999, recently rediscovered[1] by Sun, Ko, Dönigus 2019; Blum & Takimoto 2019)

$$\langle \mathcal{C}_A \rangle (\boldsymbol{P}) \equiv \langle \mathcal{C}_A(R,P) \rangle_\Sigma = \frac{\int_\Sigma P\cdot d^3\sigma(R)\, f_n^{A-Z}(R,P/A)\, f_p^Z(R,P/A)\, \mathcal{C}_A(R,P)}{\int_\Sigma P\cdot d^3\sigma(R)\, f_n^{A-Z}(R,P/A)\, f_p^Z(R,P/A)},$$

$$\approx e^{-B/T} \Big/ \Big[\Big(1+\frac{2}{3}\frac{r^2_{A,\mathrm{rms}}}{\mathcal{R}^2_\perp(M_\perp/A)}\Big)\Big(1+\frac{2}{3}\frac{r^2_{A,\mathrm{rms}}}{\mathcal{R}^2_\parallel(M_\perp/A)}\Big)^{1/2}\Big]^{(A-1)}$$

$B = M_A - Am < 0$ is the binding energy of the nuclear cluster; $M_\perp/A \approx m_\perp$ is the transverse mass of the coalescing nucleons. $\mathcal{C}_A(R,P)$ is obtained by folding the internal Wigner density of the cluster with the phase-space densities of the coalescing nucleons; for example, for deuterons

$$\mathcal{C}_\mathrm{d}(R,P) = \int \frac{d^3q\, d^3r}{(2\pi)^3}\, \mathcal{D}(\boldsymbol{r},\boldsymbol{q})\, \frac{f_p(R_+,P_+)\, f_n(R_-,P_-)}{f_p(R,P/2)\, f_n(R,P/2)}$$

$$\approx \int d^3r\, |\phi_d(\boldsymbol{r})|^2\, \frac{f_p(R_+,P/2)\, f_n(R_-,P/2)}{f_p(R,P/2)\, f_n(R,P/2)}$$

where $\mathcal{D}(\boldsymbol{r},\boldsymbol{q}) = 8\,\exp(-\boldsymbol{r}^2/d^2 - \boldsymbol{q}^2 d^2)$, with $d = \sqrt{8/3} r_{d,\mathrm{rms}} = 3.2\,\mathrm{fm}$, is the deuteron internal Wigner density in its rest frame, $R^0_\pm = R^0_d \pm \boldsymbol{u}_d\cdot\boldsymbol{r}$, $\boldsymbol{R}_\pm = \boldsymbol{R} \pm \frac{1}{2}\big(\boldsymbol{r} + \frac{\boldsymbol{u}_d\cdot\boldsymbol{r}}{1+u^0_d}\boldsymbol{u}_d\big)$, $\boldsymbol{u}_d = \boldsymbol{P}/m_d$, and similarly for $P_\pm$.

[1] up to flow effects which cause the M_T-dependence of the HBT radii and affect the spectral slopes

The quantum mechanical correction factor: Confirmation by ALICE

Sun, Ko, Dönigus 2019

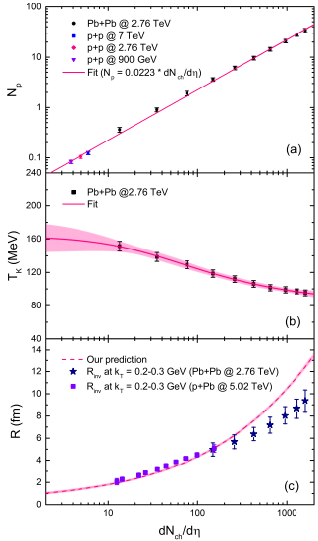

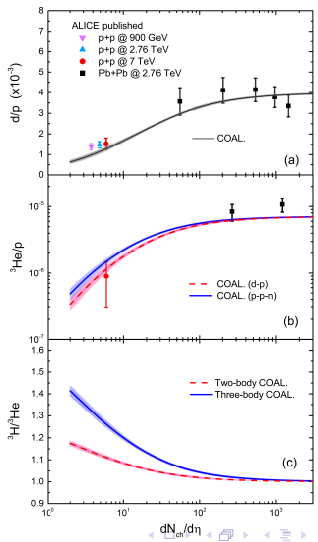

The quantum mechanical correction factor: prediction for the hypertriton

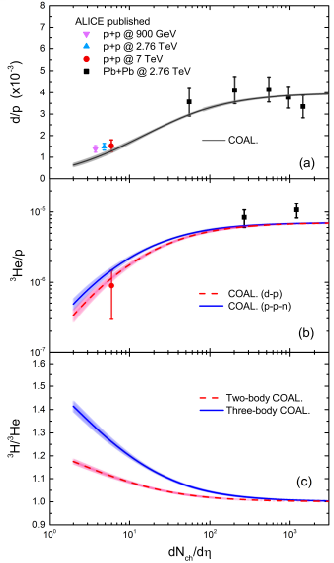

Sun, Ko, Dönigus 2019

$$S_3 = {}^3_\Lambda\mathrm{H}/\left({}^3\mathrm{He}\times\Lambda/\mathrm{p}\right)$$

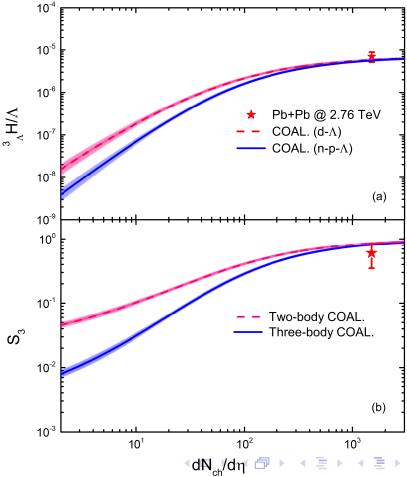

Main results: 2. The invariant coalescence factor: flow effects

By dividing the invariant cluster spectrum by the appropriate powers of the invariant nucleon spectra one obtains

$$B_A(P) = \frac{2J_A+1}{2^A}\,\langle \mathcal{C}_A \rangle\,\frac{M_\perp V_{\rm eff}(A,M_\perp)}{m_\perp V_{\rm eff}(1,m_\perp)}\left(\frac{(2\pi)^3}{m_\perp V_{\rm eff}(1,m_\perp)}\right)^{A-1} e^{(M_\perp - Am)\left(\frac{1}{T_p^*(m_\perp)}-\frac{1}{T_A^*(M_\perp)}\right)}$$

where T_p^*, T_A^* are the inverse slope parameters ("flow-boosted effective temperatures") of the nucleon and cluster spectra, and the effective volume $V_{\rm eff}$ is given by

$$V_{\rm eff}(A,M_\perp) = \frac{V_{\rm eff}(1,m_\perp)}{A^{3/2}} = \left(\frac{2\pi}{A}\right)^{3/2} V_{\rm hom}(m_\perp) \quad \Longrightarrow \quad \frac{M_\perp V_{\rm eff}(A,M_\perp)}{m_\perp V_{\rm eff}(1,m_\perp)} = 1/\sqrt{A}$$

in terms of the **homogeneity volume** $V_{\rm hom}(m_\perp) = \mathcal{R}_\perp^2(m_\perp)\,\mathcal{R}_\parallel(m_\perp)$ where $\mathcal{R}_{\perp,\parallel}(m_\perp)$ are the transverse ("sideward") and longitudinal HBT radii measured for pairs of particles with transverse mass $m_\perp$:

$$\mathcal{R}_\perp(m_\perp) = \frac{\Delta\rho}{\sqrt{1+(m_\perp/T)\eta_f^2}}, \qquad \mathcal{R}_\parallel(m_\perp) = \frac{\tau_0\,\Delta\eta}{\sqrt{1+(m_\perp/T)(\Delta\eta)^2}}.$$

Here $\Delta\rho$, $\Delta\eta$ are the geometric (Gaussian) fireball widths in transverse (radial) and longitudinal (space-time rapidity) directions, τ_0 is the nucleon kinetic freeze-out time, and η_f and $\Delta\eta = (\tau_0\Delta\eta)/\tau_0$ are the transverse and longitudinal flow velocity **gradients**.

- Connection with recent work by Blum & Takimoto 2019 will be discussed further below.

Coalescence, flow, HBT, and all that ...

The model emission function (Csörgő and Lörstad 1996)

Assumption: simultaneous **kinetic** freeze-out of pions, kaons, and nucleons and coalescence of nuclei on a common "last scattering surface" Σ_f characterized by a position-dependent freeze-out time $t_f(\boldsymbol{x})$.

Coordinate system: Milne (τ, η) and transverse polar (ρ, ϕ) coordinates:

$$R^\mu = (\tau \cosh\eta, \rho\cos\phi, \rho\sin\phi, \tau\sinh\eta)$$

Additional simplifications:

1. azimuthal symmetry ($b = 0$ collisions);
2. boost-invariant longitudinal flow rapidity $\eta_l(\tau, \rho, \eta) = \eta$ (Bjorken scaling);
3. linear transverse flow rapidity profile $\eta_\perp(\tau, \rho, \eta) = \eta_f \frac{\rho}{\Delta\rho}$;
   $u^\mu(R) = \cosh\eta_\perp(\cosh\eta, \tanh\eta_\perp\cos\phi, \tanh\eta_\perp\sin\phi, \sinh\eta)$;
4. sudden freeze-out at constant longitudinal proper time τ_0 and temperature T:
   $P\cdot d^3\sigma(R) = \tau_0 m_\perp \cosh(\eta - Y)\,\rho\, d\rho\, d\phi\, d\eta$;
5. Boltzmann approximation for nucleons and nuclei:[2]

$$f_i(R,P) = e^{\mu_i/T}\, e^{-P\cdot u(R)/T}\, H(R), \quad i = p, n;$$

$$H(R) = H(\eta,\rho) = N \exp\left(-\frac{\rho^2}{2(\Delta\rho)^2} - \frac{\eta^2}{2(\Delta\eta)^2}\right).$$

[2] Flow velocity $u^\mu(R)$ missing in Sun, Ko, Dönigus 2019, Blum & Takimoto 2019

Cluster spectra: thermal emission vs. coalescence

Thermal cluster emission: $\mu_A = Z\mu_p + (A-Z)\mu_n$

$$E\frac{d^3N_A}{d^3P} = \frac{2J_A+1}{(2\pi)^3} e^{\mu_A/T} \int_{\Sigma_f} P\cdot d^3\sigma(R)\, e^{-P\cdot u(R)/T}\, H(R)$$

Classical coalescence (pointlike nucleons and clusters, ignoring cluster binding energy):

$$E\frac{d^3N_A}{d^3P} = \frac{2J_A+1}{(2\pi)^3} e^{\mu_A/T} \int_{\Sigma_f} P\cdot d^3\sigma(R)\, e^{-P\cdot u(R)/T}\, \big(H(R)\big)^A$$

Quantum coalescence:

$$\begin{aligned} E\frac{d^3N_A}{d^3P} &= \frac{2J_A+1}{(2\pi)^3} e^{\mu_A/T} \int_{\Sigma_f} P\cdot d^3\sigma(R)\, e^{-P\cdot u(R)/T}\, \big(H(R)\big)^A \mathcal{C}_A(R,P) \\ &\approx \frac{2J_A+1}{(2\pi)^3} e^{\mu_A/T} \langle \mathcal{C}_A\rangle(P) \int_{\Sigma_f} P\cdot d^3\sigma(R)\, e^{-P\cdot u(R)/T}\, \big(H(R)\big)^A \end{aligned}$$

For freeze-out at constant density, temperature & chemical potential: $H(R) = \text{const.} = 1 = \big(H(R)\big)^A$ on Σ_f $\Longrightarrow$ **thermal emission and classical coalescence give identical results** while quantum coalescence gives slightly smaller yields (15-20% effect for deuterons from AuAu, PbPb).

Gaussian $H(R)$: **thermal** cluster emission spectrum

Using saddle point integration one obtains for the Gaussian profile function $H(R)$ (Scheibl & Heinz 1999)

$$E\frac{d^3N_A}{d^3P} = \frac{2J_A+1}{(2\pi)}\, e^{(\mu_A - M)/T} M_\perp V_{\rm eff}(1, M_\perp) \exp\left(-\frac{M_\perp - M}{T_A^*} - \frac{Y^2}{2(\Delta\eta)^2}\right)$$
$$= \frac{2J_A+1}{(2\pi)^{3/2}}\, e^{(\mu_A - M)/T} M_\perp V_{\rm hom}(M_\perp) \exp\left(-\frac{M_\perp - M}{T_A^*} - \frac{Y^2}{2(\Delta\eta)^2}\right)$$

with an inverse slope parameter ("effective temperature") that increases linearly with the cluster mass:

$$T_A^* = T + M\,\eta_f^2.$$

Gaussian $H(R)$: spectrum from **classical coalescence**

Using saddle point integration one obtains for the Gaussian profile function $H(R)$

$$E\frac{d^3N_A}{d^3P} = \frac{2J_A+1}{(2\pi)}\, e^{(\mu_A - Am)/T} M_\perp V_{\rm eff}(A, M_\perp) \exp\left(-\frac{M_\perp - Am}{T_A^*} - \frac{AY^2}{2(\Delta\eta)^2}\right)$$
$$= \frac{2J_A+1}{(2\pi)^{3/2}}\, e^{(\mu_A - Am)/T} M_\perp \frac{V_{\rm hom}(m_\perp)}{A^{3/2}} \exp\left(-\frac{M_\perp - Am}{T_A^*} - \frac{AY^2}{2(\Delta\eta)^2}\right)$$

where $M_\perp \equiv \sqrt{(Am)^2 + P_\perp^2}$, with an inverse slope parameter ("effective temperature") **independent of cluster size:**

$$T_A^* = T + \frac{Am}{A}\eta_f^2 = T + m\,\eta_f^2 = T_p^*.$$

This is clearly a deficiency of the assumed Gaussian transverse density profile in this toy model.

Freeze-out at constant density eliminates this difference and thus corrects this deficiency.

Note that $M = Am + B$ where binding energy $|B| \ll T$ is negligible.

Gaussian $H(R)$: spectrum from **quantum coalescence**

Using saddle point integration one obtains for the Gaussian profile function $H(R)$

$$E\frac{d^3N_A}{d^3P} = \frac{2J_A+1}{(2\pi)}\, e^{(\mu_A - Am)/T}\langle \mathcal{C}_A\rangle(P)\, M_\perp\, V_{\rm eff}(A, M_\perp)\exp\left(-\frac{M_\perp - Am}{T_A^*} - \frac{AY^2}{2(\Delta\eta)^2}\right)$$
$$= \frac{2J_A+1}{(2\pi)^{3/2}}\, e^{(\mu_A - Am)/T}\langle \mathcal{C}_A\rangle(P)\, M_\perp\, \frac{V_{\rm hom}(m_\perp)}{A^{3/2}}\exp\left(-\frac{M_\perp - Am}{T_A^*} - \frac{AY^2}{2(\Delta\eta)^2}\right)$$

where $M_\perp \equiv \sqrt{(Am)^2 + P_\perp^2}$, with an inverse slope parameter ("effective temperature") independent of cluster size:

$$T_A^* = T + \frac{Am}{A}\eta_f^2 = T + m\,\eta_f^2 = T_p^*.$$

Compared to classical coalescence, the only difference is the quantum mechanical suppression factor $\langle C_A\rangle(P)$.

Again, the problem with nuclei and protons having the same predicted inverse slope goes away for freeze-out at constant density, $H(R) = 1$.

Coalescence, flow, HBT, and all that ...

Chemical vs. kinetic decoupling of light nuclei: PCE BW model

Xu & Rapp, 1809.04024 (EPJ A55 ('19) 68):

Nuclei yields and p_T-spectra from STAR and ALICE can be understood in terms of thermal production (=classical coalescence!) at $T_{\rm chem} = 160\,{\rm MeV}$ and $T_{\rm kin} = 100\,{\rm MeV}$, with $\beta_s = 0.780\,(0.866)$ at RHIC (LHC) (blast wave parametrization):

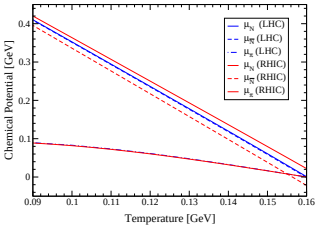

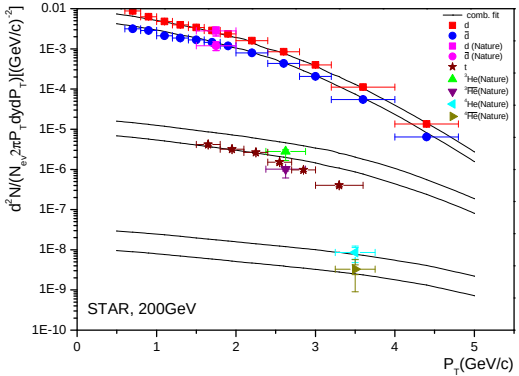

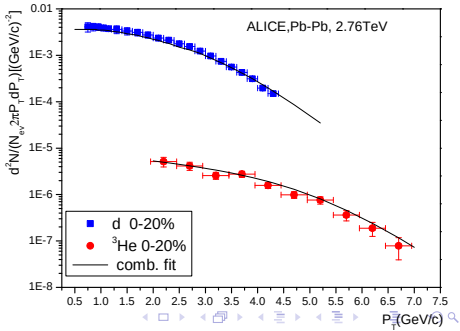

Chemical vs. kinetic decoupling of light nuclei: BW model (ALICE version)

Consistent with earlier ALICE analysis:

ALICE 1506.08951 (PRC 93 (2015) 024917):

Hadron and nuclei p_T-spectra from ALICE can be understood in terms of common kinetic freeze-out (=classical coalescence!) at $T_{\rm kin} = 113 \pm 12$ MeV, with $\langle\beta\rangle = 0.632 \pm 0.010$ (blast wave parametrization):

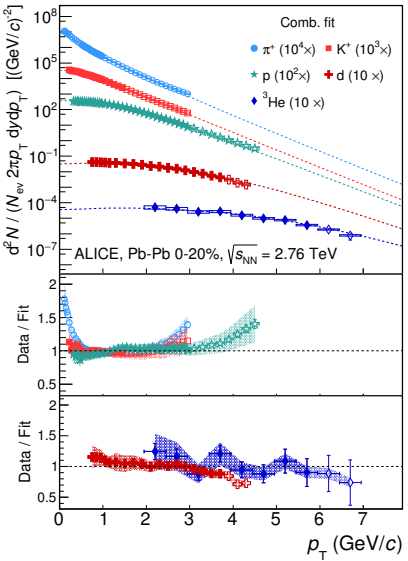

Chemical vs. kinetic decoupling of light nuclei: hadronic Saha equation (PCE)

Vovchenko et al. 1903.10024 (PLB 800 (2020) 135131):

Partial chemical equilibrium $p + n + \pi \leftrightarrow d + \pi$ gives

$$\frac{N_A(T)}{N_A(T_{\rm ch})} \simeq \left(\frac{T}{T_{\rm ch}}\right)^{\frac{3}{2}(A-1)} \exp\left[B_A\left(\frac{1}{T}-\frac{1}{T_{\rm ch}}\right)\right]$$

$$\neq \left(\frac{T}{T_{\rm ch}}\right)^{-\frac{3}{2}} \exp\left[-m_A\left(\frac{1}{T}-\frac{1}{T_{\rm ch}}\right)\right].$$

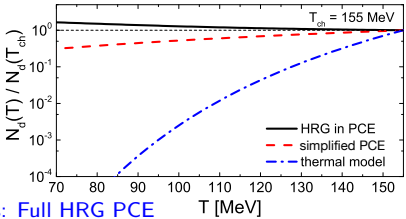

Colored bands: ALICE data Lines: Full HRG PCE

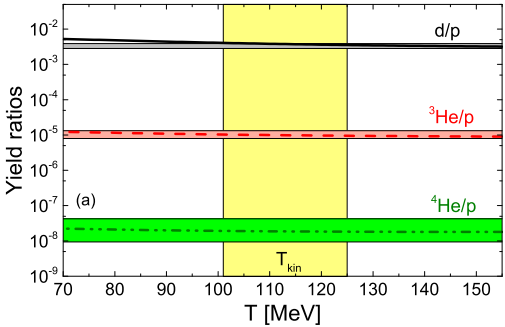

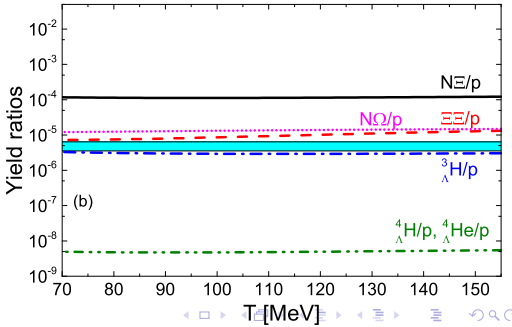

Chemical vs. kinetic decoupling of deuterons: hydro+UrQMD:

Sombun et al. PRC99 ('19) 014901; Stock et al., NPA 982 ('19) 2019

Yields calculated from hydro + UrQMD hybrid simulation, with final state coalescence implemented in UrQMD, agree with ALICE data and with Statistical Hadronization Model + UrQMD.

Statistical Hadronization Model with the same chemical freeze-out parameters but without UrQMD rescattering (i.e. w/o p-$\bar{\text{p}}$ annihilation through FSI) disagrees with the data and full dynamical simulations.

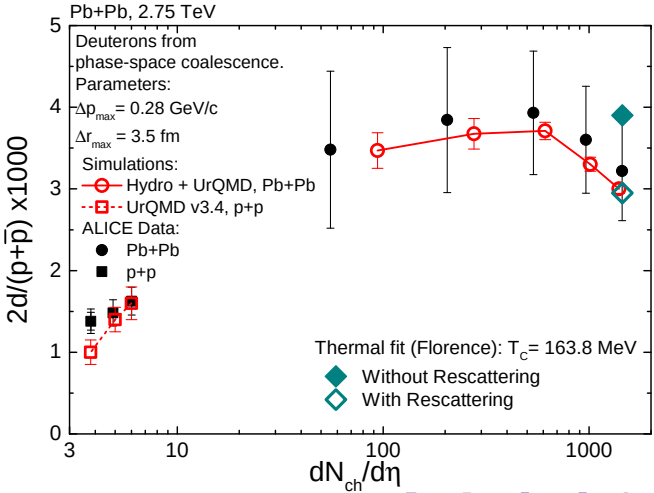

Chemical vs. kinetic decoupling of deuterons: hydro+SMASH

Oliinychenko, Pang, Elfner, Koch, 1809.03071 (TRENTO+CLVisc+SMASH)

Incorporate $\pi d \leftrightarrow \pi np$ with detailed balance in the SMASH afterburner ("pion catalyzed coalescence"):

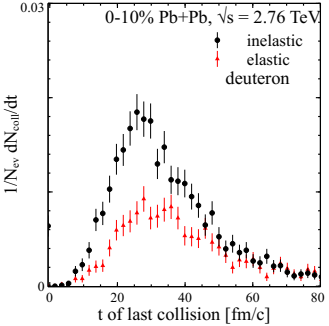

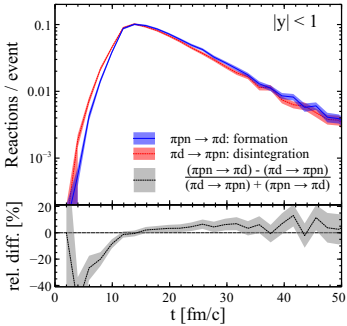

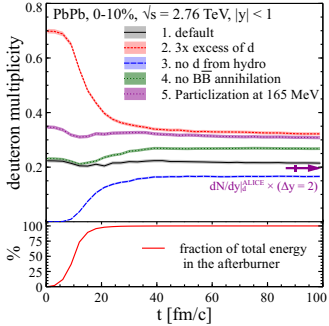

Chemical freeze-out of deuterons occurs about $> 10\,\mathrm{fm}/c$ after completion of hadronization process.
At that point, $> 99\%$ of deuterons originally produced at $T_{\mathrm{chem}} = 160\,\mathrm{MeV}$ have been destroyed;
$\approx$ all experimentally observed deuterons are created in SMASH via $\pi np \to \pi d' \to \pi d$ ("coalescence").

Coalescence parameter B_2 in TRENTO+CLVisc+SMASH:

Oliinychenko, Pang, Elfner, Koch, PRC99 ('19) 044907

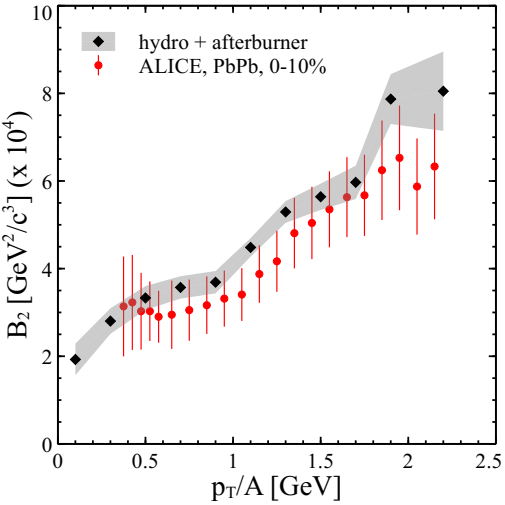

$B_2(p_T)$ increases with p_T, as qualitatively predicted by the toy model coalescence calculation in Scheibl & Heinz 1999 and in agreement with ALICE data.

TRENTO+hydro+SMASH also correctly describes the p_T-spectra of π, K, p and d (and antiparticles), but calculation has insufficient statistics to check deuteron elliptic flow v_2^d.

Coalescence, flow, HBT, and all that ...

Cluster spectra from wave function overlap

Danielewicz and Schuck 1992 [PLB 274 (1992) 268]:

In the cluster rest frame, coalescence is a non-relativistic process. Starting from the square of the overlap matrix element between the deuteron wave function and those of a proton and a neutron and rewriting it in terms of density matrices and ultimately Wigner densities, Danielewicz and Schuck showed that in the deuteron rest frame the deuteron momentum spectrum can be calculated as

$$\frac{dN_d}{d^3P_d} = \frac{-3i}{(2\pi)^3}\int d^4r_{\rm cl}\, d^3r \int \frac{d^4p_1}{(2\pi)^4}\,\frac{d^3p_2}{(2\pi)^3}\,(2\pi)^4\delta^4(P_d - p_1^* - p_2)$$
$$\times \mathcal{D}\left(\boldsymbol{r}, \tfrac{\boldsymbol{p}_1-\boldsymbol{p}_2}{2}\right)\left[\Sigma_p^<(p_1^*, r_+)\, f_n^W(p_2, r_-) + \Sigma_n^<(p_1^*, r_+)\, f_p^W(p_2, r_-)\right],$$

where p^* denotes an off-shell momentum, due to a preceding collision of the off-shell particle with a third body. The energy-momentum conserving δ-function can only be satisfied if either the neutron or the proton is off-shell.

Cluster spectra from wave function overlap

The off-shell nucleon self energy is given by

$$
\begin{aligned}
-i\Sigma_N^<(p^*,x) &= \sum_j \int \frac{d^3q}{(2\pi)^3}\,\frac{d^3p'}{(2\pi)^3}\,\frac{d^3q'}{(2\pi)^3}(2\pi)^4\delta^4(p^*+q-p'-q') \\
&\qquad \times |M_{Nj\to Nj}|^2 f_N^W(p',x)\, f_j^W(q',x)\,\left(1\pm f_j^W(q,x)\right) \\
&\approx f_N(p^*,x)\sum_j \int \frac{d^3q}{(2\pi)^3}\, f_j(q,x) \\
&\qquad \times \Big[\int \frac{d^3p'}{(2\pi)^3}\,\frac{d^3q'}{(2\pi)^3}\,(2\pi)^4\delta^4(p^*+q-p'-q')|M_{Nj\to Nj}|^2\,\left(1\pm f_j(q',x)\right)\Big] \\
&= \frac{f_N(p^*,x)}{\tau^N_{\rm scatt}(\boldsymbol{p},x)}\,.
\end{aligned}
$$

Deuterons have twice the scattering rate of their constituent nucleons. Since any scattering is likely to break up the deuteron, the integration over $t_d = r_d^0$ in the deuteron rest frame should only go from $t_f - \frac{1}{2}\tau^N_{\rm scatt}$ to t_f. Assuming the scattering time to be sufficiently short to neglect any change in the distribution functions during this time interval the factors of $\tau^N_{\rm scatt}$ cancel, and ...

Cluster spectra from wave function overlap

. . . we get

$$\frac{dN_d}{d^3P_d} = \frac{3}{(2\pi)^3} \int d^3r_d \int \frac{d^3r\, d^3q}{(2\pi)^3}\, \mathcal{D}(\boldsymbol{r},\boldsymbol{q})\, f_p(q_+, r_+)\, f_n(q_-^*; r_-)$$

where

$$q_+^\mu = \left(\sqrt{m^2+\boldsymbol{q}^2},\, \boldsymbol{q}\right), \qquad q_-^{*\mu} = \left(M_d - \sqrt{m^2+\boldsymbol{q}^2},\, -\boldsymbol{q}\right).$$

Lorentz transforming this to the global frame by Lorentz-boosting the rest-frame positions and momenta with the four-velocity of the deuteron, we can use $E_d d^3r_d = P_d \cdot d^3\sigma(R_d)$ and write this as

$$E_d \frac{dN_d}{d^3P_d} = \frac{3}{(2\pi)^3} \int_{\Sigma_f} P_d \cdot d^3\sigma(R_d)\, f_p(R_d, P_d/2)\, f_n(R_d, P_d/2)\, \mathcal{C}_d(R_d, P_d)$$

which defines the previously listed quantum mechanical correction factor $\mathcal{C}_d(R_d, P_d)$.

The quantum mechanical correction factor

Some typical values for the quantum mechanical correction factor for deuterons from AuAu, PbPb collisions using the Gaussian emission function model are listed in the following Table:

TABLE I. The quantum-mechanical correction factor $\mathcal{C}_d^0$ for Hulthen and harmonic oscillator wave functions calculated with Eq. (3.21), for different fireball parameters at nucleon freeze-out (for details see text).

τ_0 [fm/c]		9.0			6.0	
T [MeV]	168	130	100	168	130	100
η_f	0.28	0.35	0.43	0.28	0.35	0.43
Hulthen	0.86	0.84	0.80	0.80	0.78	0.74
harm. osc.	0.84	0.81	0.76	0.76	0.72	0.66

Note that the more realistic Hulthen wave function, which (in spite of the same $r_{\rm rms}$) peaks at a smaller value of r than the Gaussian, has better overlap with the "homogeneity factor" $f(R_+, P/2)f(R_-, P/2)/f^2(R, P/2)$ than the Gaussian one, because the latter peaks strongly at $r = 0$.

Coalescence, flow, HBT, and all that ...

Coalescence and femtoscopy:

Extending work by Mrowczynski '87-'93, Blum & Takimoto [PRC 99 ('19) 044913] established a direct connection between the B_2 value for deuterons and the pp quantum statistical (FD) correlation function $C_2(K,q) = 1 - \frac{3}{4}\mathcal{C}_2(K,q)$:

$$B_2(K) \approx \frac{3}{2m}\int d^3\bar{q}\,\mathcal{D}(\bar{\boldsymbol{q}})\,\mathcal{C}_2(\bar{\boldsymbol{K}},\bar{\boldsymbol{q}})$$

Here $(\bar{\boldsymbol{K}},\bar{\boldsymbol{q}})$ are the proton pair and relative momenta in the pair rest frame, and $\mathcal{C}_2$ is assumed to have been corrected experimentally for strong FSI.

Assuming a Gaussian form $\mathcal{C}_2(\bar{K},\bar{q}) = \lambda e^{-\bar{\mathcal{R}}^2_\perp(\bar{K})\bar{q}^2_\perp - \bar{\mathcal{R}}^2_\parallel(\bar{K})\bar{q}^2_l}$ in the pair rest frame they find

$$B_2 = \frac{3\pi^{3/2}\lambda}{2m\left(\bar{\mathcal{R}}^2_\perp + \frac{2}{3}r^2_{d,\mathrm{rms}}\right)\left(\bar{\mathcal{R}}^2_\parallel + \frac{2}{3}r^2_{d,\mathrm{rms}}\right)^{1/2}}$$

$$\frac{B_A}{m^{2(A-1)}} = \lambda^{A/2}\frac{2J_A}{2^A\sqrt{A}}\left[\frac{(2\pi)^{3/2}}{m^3\left(\bar{\mathcal{R}}^2_\perp + \frac{2}{3}r^2_{A,\mathrm{rms}}\right)\left(\bar{\mathcal{R}}^2_\parallel + \frac{2}{3}r^2_{A,\mathrm{rms}}\right)^{1/2}}\right]^{A-1}$$

λ accounts for unresolved resonance decay contributions in the denominator of $\mathcal{C}_2$.

Note that $m\bar{\mathcal{R}}_\perp = m_\perp\mathcal{R}_\perp$ (transverse boost from lab frame to pair rest frame), so the dependence on correlation radii agrees with Scheibl & Heinz '99. B&T's result clarifies that the QM correction factor $\langle\mathcal{C}_A\rangle$ depends on the ratio between cluster and homogeneity radii in the cluster rest frame.

$B_{2,3}$ from spectra vs. $\mathcal{R}$ from femtoscopy: ALICE @ LHC

Blum & Takimoto PRC 99 ('19) 044913, assuming $\mathcal{R}_\perp = \mathcal{R}_\parallel = R$

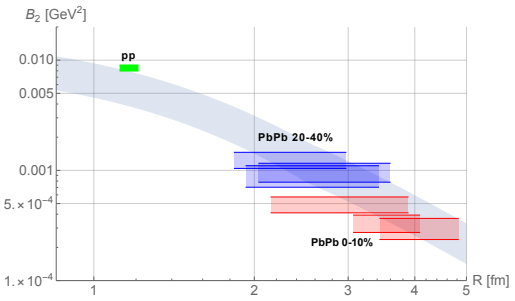

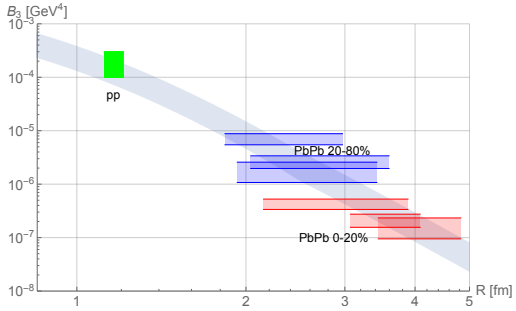

Different bars with the same color correspond to different $m_\perp$ bins within a centrality class.

But what about the flow correction factor $e^{(M_\perp - M)\left(\frac{1}{T_p^*(m_\perp)} - \frac{1}{T_A^*(M_\perp)}\right)}$ **?**

$B_{2,3}$ from spectra vs. $dN_{\rm ch}/d\eta$

Popular[3] proxy for $V_{\rm hom}(m_\perp) = \mathcal{R}^2_\perp(m_\perp)\,\mathcal{R}_\parallel(m_\perp)$: $V_{\rm hom} \propto dN_{\rm ch}/d\eta$.

ALICE 2003.03184

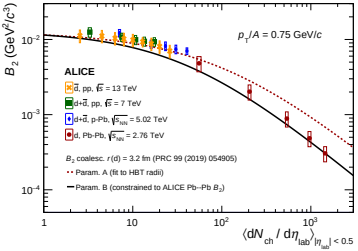

ALICE 1910.14401 (PRC 101 (2020) 044906)

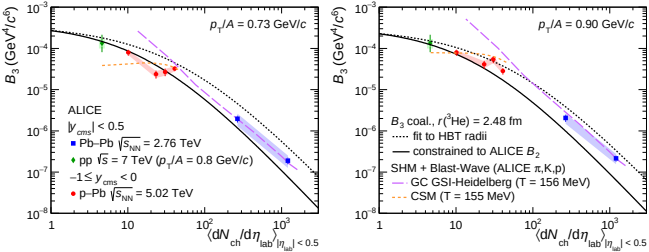

But this proxy neglects all kinds of momentum and collision system dependences!

[3] among experimentalists

HBT homogeneity volume ↔ charged multiplicity?

Data show that, at fixed $k_\perp$, $V_{\rm hom} = \mathcal{R}_\perp^2\,\mathcal{R}_\parallel \propto dN_{\rm ch}/d\eta$, but that the **proportionality constant depends on the size of the collision system** (red dots: pPb; green squares: pp; others: PbPb/AuAu/CuCu):

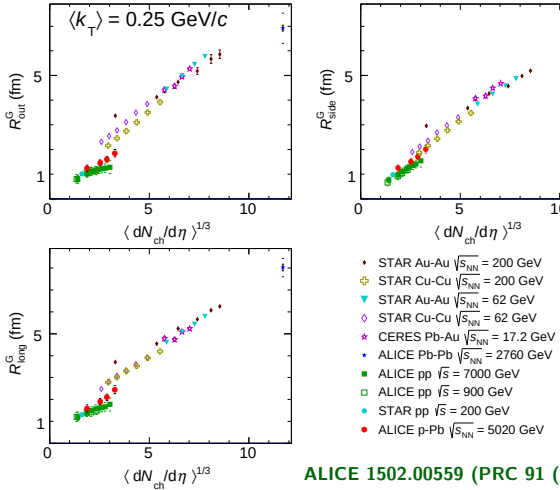

In smaller systems, a more compact initial configuration implies larger density gradients which cause stronger radial flow.

This reduces the HBT radii in small systems relative to those in large systems at the same multiplicity.

ALICE 1502.00559 (PRC 91 (2015) 034906)

Coalescence, flow, HBT, and all that ...

Summary (in the form of qualitative predictions from the coalescence model):

- **Thermal production of nuclear clusters at $T_{\rm chem} \simeq 160$ MeV is logically untenable**. All such produced clusters get destroyed by subsequent hadronic rescattering whose effects are seen in the cluster momentum distributions. Clusters form by coalescence at the end of this rescattering stage.

- For kinetic freeze-out at constant T and μ (and thus at constant particle and energy density) **classical coalescence produces the same particle yields and spectra as the thermal model**, **independent of the value of the kinetic freeze-out temperature**. Just as the chemical temperature extracted from elementary hadron yield ratios provides no information about their kinetic freeze-out temperature, the chemical temperature extracted from particle ratios involving nuclear clusters provides no information about the temperature at which the coalescence process took place.

- Quantum mechanical effects, which scale with the ratio of the intrinsic cluster volume divided by the homogeneity volume of the coalescing nucleons (which can be extracted from femtoscopic measurements), **suppress** deuteron yields by 15-25% in collisions between large nuclei and by larger factors in smaller and more rapidly expanding systems. Binding energy correction effects are typically small (^{4}He?).

- The invariant coalescence factors $B_A \sim e^{(M_\perp - Am)\left(\frac{1}{T_p^*(m_\perp)} - \frac{1}{T_A^*(M_\perp)}\right)} \Big/ \sqrt{A}\left(m_\perp V_{\rm hom}(m_\perp)\right)^{A-1}$ **increase** with $m_\perp$ (due to the corresponding **decrease** of the HBT homogeneity volume and the flow-induced slope-difference of the nucleon and nuclei transverse momentum spectra) and **decrease** with $\sqrt{s}$ (due to the corresponding **increase** of the HBT homogeneity volume, reflecting smaller radial flow *gradients* at freeze-out), qualitatively consistent with observations.

Thank you!

Extra slides

B_2 from femtoscopy vs. ratio of spectra: Pb-Pb @ LHC

Blum & Takimoto PRC 99 ('19) 044913, assuming $\mathcal{R}_\perp = \mathcal{R}_\parallel = R$

central Pb-Pb (0-10%)

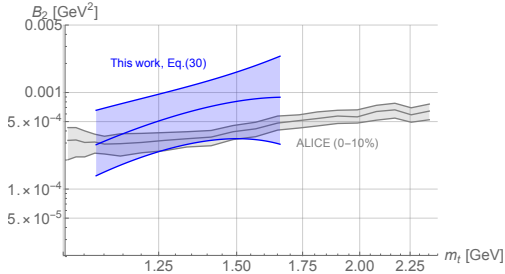

semi-peripheral Pb-Pb (20-60%)

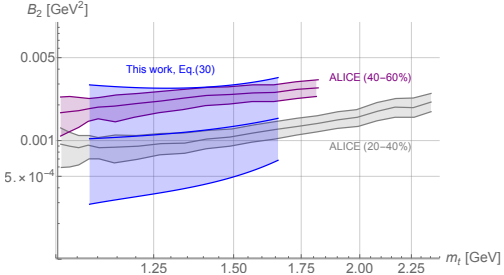

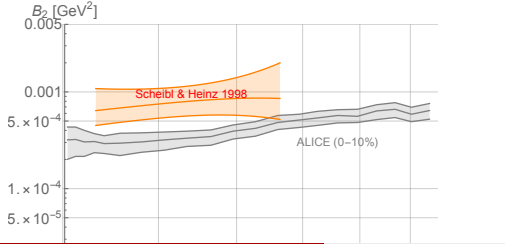

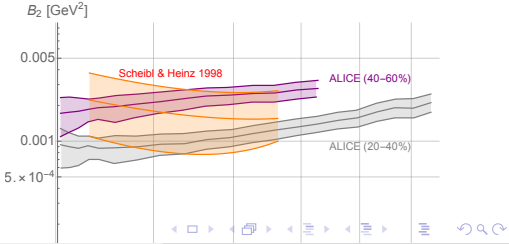

B_3 from femtoscopy vs. ratio of spectra: Pb-Pb @ LHC

Blum & Takimoto PRC 99 ('19) 044913, assuming $\mathcal{R}_\perp = \mathcal{R}_\parallel = R$

central Pb-Pb (0-20%)

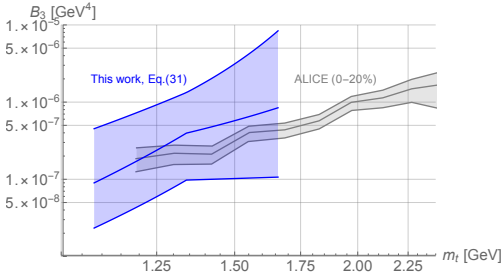

peripheral Pb-Pb (20-80%)